JACS JOURNAL OF THE AMERICAN CHEMICAL SOCIETY

Article

pubs.acs.org/JACS

New Mechanism for Photocatalytic Reduction of CO_2 on the Anatase TiO_2(101) Surface: The Essential Role of Oxygen Vacancy

Yongfei Ji[†,‡] and Yi Luo*[,†,‡]

[†]Hefei National Laboratory for Physical Science at the Microscale and Synergetic Innovation Center of Quantum Information & Quantum Physics, University of Science and Technology of China, Hefei, 230026 Anhui, PR China

[‡]Department of Theoretical Chemistry and Biology, School of Biotechnology, Royal Institute of Technology, S-106 91 Stockholm, Sweden

Supporting Information

ABSTRACT: Photocatalytic reduction of CO_2 into organic molecules is a very complicated and important reaction. Two possible pathways, the fast-hydrogenation (FH) path and the fast-deoxygenation (FdO) path, have been proposed on the most popular photocatalyst TiO_2. We have carried out first-principles calculations to investigate both pathways on the perfect and defective anatase TiO_2(101) surfaces to provide comprehensive understanding of the reaction mechanism. For the FH path, it is found that oxygen vacancy on defective surface can greatly lower the barrier of the deoxygenation processes, which makes it a more active site than the surface Ti. For the FdO path, our calculation suggests that it can not proceed on the perfect surface, nor can it proceed on the defective surface due to their unfavorable energetics. Based on the fact that the FH path can proceed both at the surface Ti site and the oxygen vacancy site, we have proposed a simple mechanism that is compatible with various experiments. It can properly rationalize the selectivity of the reaction and greatly simplify the picture of the reaction. The important role played by oxygen vacancy in the new mechanism is highlighted and a strategy for design of more efficient photocatalysts is proposed accordingly.

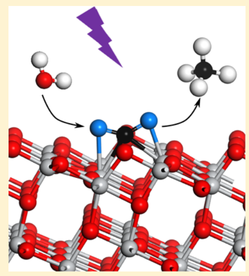

■ INTRODUCTION

Photocatalytic reduction of CO_2 to solar fuels is a promising solution for the energy crisis and global warming. Depending on the number of electrons and protons transferred, CO_2 can be reduced to HCOOH, CO, CH_2O, CH_3OH, and CH_4, respectively. Numerous studies have been carried out on the most popular photocatalysts, namely, TiO_2.[1−6] The reaction turns out to be very complicated, and its mechanism is still not well understood. The most puzzling result is that the product distribution seems to depend sensitively on the experimental details[3,5,7] with no easy way to understand the selectivity. Although the product is usually a combination of CH_4, CH_3OH, and CO, each of the C1 molecules has been identified as the major product by different experiments, sometimes with no traces of other species.[3,5,7,8] To explain the experimental results, two pathways (Scheme 1) have been proposed depending on whether the hydrogenation or the deoxygenation process is faster.[2,5] In the fast-hydrogenation (FH) pathway, which is also called formaldehyde pathway, CO_2 is reduced along the path $CO_2 \rightarrow HCOOH \rightarrow CH_2O \rightarrow CH_3OH \rightarrow CH_4$; in the fast-deoxygenation (FdO) pathway (also called carbene pathway), it follows the path $CO_2 \rightarrow CO \rightarrow C^{\cdot} \rightarrow CH_3^{\cdot} \rightarrow CH_3OH/CH_4$. The intermediates in both pathways have been detected in some but not all experiments.[2,5,9,10] The FH path is thermodynamically feasible. However, CH_3OH appears as an intermediate not a product which is the reason why the kinetic model based on the FH path can not explain the product concentration profile observed in experiments.[11,12] It also does not agree with the experiment, in which CH_3OH and

Scheme 1. Proposed Pathways for the Photocatalytic Reactions on the Perfect and Defective Surfaces[a]

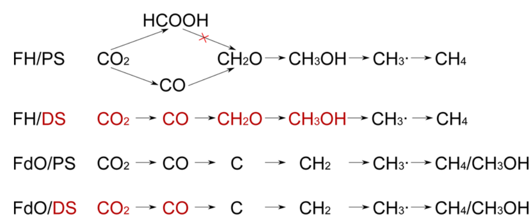

[a]FH: fast-hydrogenation path; FdO: fast-deoxygenation path; PS: perfect surface; DS: defective surface. Red species are adsorbed at oxygen vacancy and black ones on Ti.

CH_4 appear simultaneously rather than consecutively.[11] The FdO path does not have this problem because CH_3OH always appears as one of the final products,[11,12] but the possible formation of formic acid and formaldehyde are obviously not included in it. A compatible explanation for all the experiments is that the reaction may proceed via both pathways, and the final products may depend on which one is the dominating one. Although it is convenient to divide the reaction into these two categories, none of the them has been directly verified by experiments. Furthermore, it cannot explain why or predict when one of the pathway will dominate.

Received: June 3, 2016
Published: November 21, 2016

DOI: 10.1021/jacs.6b05695
J. Am. Chem. Soc. 2016, 138, 15896−15902

In this work, we intend to give a comprehensive understanding of the reaction and a proper mechanism to rationalize its selectivity. We assume that the reaction can proceed via both the FH and FdO pathways at more than one active sites on the surface. It implies that the final product distribution will be mainly determined by the abundances of these active sites, which in turn depends greatly on the preparation methods and experimental setups.

We have chosen the surface 5-fold coordinated surface Ti atom (Ti_{5f}) and oxygen vacancy (O_v) on the anatase $TiO_2(101)$ surface to be the active sites. The Ti_{5f} sites are abundant on the surface, and molecules can be adsorbed strongly at it. This is the reason why reactions are often expected to happen at them.[13] However, more and more experiments showed that O_v is the real active site for many reactions on TiO_2. For example, the H_2O molecule was found only to dissociate at O_v on the rutile $TiO_2(110)$ surface;[14] it is the O_2 adsorbed at O_v that is responsible for photooxidation of CO.[15] Defective surface was also found to be more active than the perfect surface for reactions such as photodecomposition of methanol,[16−18] although the exact reason for the enhancement is not known. Recently, it has been shown that[19] the production of CO and CH_4 from CO_2 photoreduction can be enhanced on defective surface by 10-fold. Therefore, to comprehensively understand the mechanism of the reaction, we have to investigate the reaction on both the perfect and defective TiO_2 surfaces, i.e., to investigate both paths at Ti_{5f} and the O_v sites.

The FH pathway on the Ti_{5f} (FH/PS) has been investigated in our previous work.[20] It was modified to $CO_2 \rightarrow CO \rightarrow CH_2O \rightarrow CH_3OH \rightarrow CH_4$ because the barrier for the reduction of HCOOH to CH_2O is very high (Scheme 1). The rate-limiting step is the deoxygenation of CO_2 to CO with a barrier of 1.41 eV. We still need to study the FH path at the O_v and the FdO path on the perfect and the defective surfaces. As shown in Scheme 1, for FH path at the O_v (FH/DS), the first four steps occur at the O_v. CO at the O_v can be hydrogenated to CH_3OH before it deoxygenates at the vacancy to produce $CH_3^{\cdot}$ with a cured O_v. Then, $CH_3^{\cdot}$ will be further hydrogenated to CH_4. It is noted that for the FdO path at the O_v of defective surface (FdO/DS) the deoxygenation of CO_2 and CO can occur at the O_v. The potential energy surface of these three paths are explored. Based on these results, we will propose a new mechanism and discuss how it can explain various experiments.

COMPUTATIONAL METHODS

The theoretical method employed here is similar to the one used in our previous work on photoreduction of CO_2 on the perfect anatase TiO_2 surface[20] through the formaldehyde pathway. All calculations have been carried out with the Vienna Ab-initio Simulation Package (VASP)[21−25] at the generalized gradient approximation (GGA) level. Ion-electron interaction was described by the PAW[26] pseudopotential with the PBE[27] functional as the exchange-correlation functional of the electrons. An energy cutoff of 460 eV was adopted for the plane-wave basis set. The anatase $TiO_2(101)$ surface was presented by a five-layer slab. A 3 × 1 supercell along [010] and $[10\bar{1}]$ directions with a vacuum layer of 13 Å was used. The system contains 180 atoms and only the Γ point was included for the sampling of Brillouin zone. Both sides of the slab were relaxed with the atoms in the center layer fixed to the bulk positions. Such a slab model has been successfully applied in our previous studies on the mechanism of several photocatalytic reactions.[20,28,29] Structures were optimized until the maximum force on the atoms was smaller than 0.02 eV/Å. Transition states were searched with the nudged elastic band method with climbing images(CNEB).[30]

$$H_2O + 2h^+ \rightarrow \frac{1}{2}O_2 + 2H^+ \quad (1)$$

$$CO_2 + 8H^+ + 8e^- \rightarrow CH_4 + 2H_2O \quad (2)$$

For the photoreduction of CO_2, protons and photoexcited electrons are both needed. In artificial photosynthesis, H_2O is suggested to be oxidized by photogenerated hole[31,32] to produce O_2 and protons[10,33] (reaction 1) which are used to reduce CO_2 with photogenerated electrons (reaction 2). In our calculations, H atoms (H_b) were adsorbed onto the surface bridging oxygen (O_b) to provide both the protons and electrons.[20,34] Photogenerated electrons on TiO_2 are supposed to undergo trapping after photogeneration.[35,36] Trapped electrons cannot be described properly by GGA because of the self-interaction error[37] in DFT. Two methods have been frequently used to overcome this problem. One is to use the DFT+U[38] method with the U corrections applied to the d-orbital of Ti atom. However, this will introduce uncontrolled error, and the results will depend on U value, which has to be scanned to see the change of related properties of the system. Another method is to use hybrid functional (such as the HSE[39]), which is more accurate but also much more time-consuming. As a compromise, we used the GGA+U/HSE method, in which the HSE functional is used to calculate the energies of the GGA+U (U = 4.0 eV) optimized structures. A test calculation has been performed in our previous work,[20] which shows that the GGA+U/HSE results are quite close to the pure HSE results, whereas the GGA+U results agree qualitatively with the HSE but might give the wrong rate-limiting step. The GGA+U results can be found in the Supporting Information.

RESULTS AND DISCUSSION

FH Path at the Oxygen Vacancy. *Reduction of CO_2 at the Oxygen Vacancy.* As shown in Scheme 1, the first step of the FH/DS path is the deoxygenation of CO_2 to CO at the O_v. Two possible pathways have been considered: the direct dissociation of CO_2 to CO and the reduction by H to CO adsorbed at the O_v (reaction 3). As shown below, our calculations suggest that direct dissociation is much more favorable.

$$CO_2 + 2H^+ + 2e^- \rightarrow CO + H_2O \quad (3)$$

Figure 1a shows the potential energy surface (PES) for the direct dissociation of CO_2. The two most stable configurations are states A and B separated by a transformation barrier of 1.04 eV. From state B, there is only a small barrier of 0.04 eV for the CO_2 molecule to dissociate to CO, resulting in a total barrier of 1.04 eV for the dissociation of CO_2. However, if CO_2 in state A dissociates via another path in which CO is produced on the other site of the O_v (state C), then the barrier is greatly reduced to 0.73 eV. The calculated structures and relative energies agree well with those of previous theoretical studies by Sorescu et al.[40]

Figure 1b shows the PES for CO_2 reduction to CO. The molecule is first hydrogenated to COOH which will further be decomposed to CO and a OH group. The barrier is calculated to be 1.19 eV for the hydrogenation and 0.1 eV for the decomposition. The reaction is slightly endothermic by 0.09 eV, but if the OH group recombines with another H to form H_2O, then the total reaction (reaction 3) will be exothermic by 0.58 eV (see Supporting Information). The barrier for the recombination of OH and H is small.[29] The rate-limiting step is the first one with a barrier of 0.45 eV higher than that for the direct dissociation, but it is still lower than the one on the

DOI: 10.1021/jacs.6b05695
J. Am. Chem. Soc. 2016, 138, 15896−15902

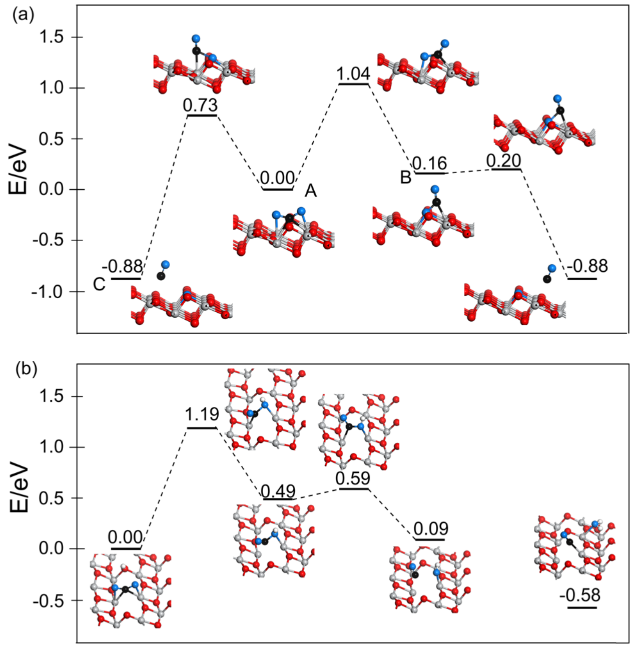

Figure 1. (a) Adsorption and direct dissociation of CO_2 at the O_v. (b) Dissociation of CO_2 via hydrogenation of CO_2 to COOH. Blue, red, gray, and black atoms are oxygen atoms of the molecule, oxygen atoms of TiO_2, Ti, and C atoms.

perfect surface,[20] implying that deoxygenation is easier at the O_v.

One may argue that CO_2 can also be reduced to formate and formic acid at the O_v. However, in state A in Figure 1a, CO_2 is bent toward the surface. It is difficult for the proton to reach the C atom of CO_2 molecule.[41] Moreover, previous experiments have shown that formic acid adsorbed at the O_v can easily dissociates to formate,[42] which suggests that even if formate can be formed at the O_v it cannot be further hydrogenated to formic acid. Therefore, the most feasible pathway for the reduction of CO_2 is the direct dissociation to CO as shown in Figure 1a.

Hydrogenation of CO. Following the FH path, CO will be further hydrogenated to CH_4. On the perfect TiO_2 surface, six protons and six electrons are needed to reduce CO to CH_4 as shown in reaction 4. Four of the protons are added to the C atom to form CH_4, and the other two recombine with the O atom to form H_2O. For the hydrogenation of CO at the O_v only four protons are needed because the O in CO molecule will remain at the O_v to cure it (reaction 5, O_b stands for bridging oxygen). We will first investigate the hydrogenation of CO to CH_3OH, then consider the formation of methyl radical and subsequent reactions.

$$CO + 6H^+ + 6e^- \rightarrow CH_4 + H_2O \quad (4)$$

$$CO + O_v + 4H^+ + 6e^- \rightarrow CH_4 + O_b^{2-} \quad (5)$$

In our calculations, hydrogens were assumed to be added one by one to the molecule. CO can then be hydrogenated to CH_3OH following four steps: CO → HCO, HCO → CH_2O, CH_2O → CH_3O, and CH_3O → CH_3OH. They are labeled as H-I to H-IV. The full PES for these reactions are shown in Figure 2.

In step H-I, CO molecule is initially adsorbed nearly vertically at the O_v with a proton adsorbed at the nearby bridging oxygen. It is transformed to an intermediate state in which CO is lying with a bridging geometry by overcoming a barrier of 0.75 eV. From the intermediate state to the final state, CO is hydrogenated to HCO by overcoming a barrier of 0.81 eV, which gives an overall barrier of 1.01 eV. Because each O_v supplies two excess electrons, CO is reduced to HCO^- anion in this step. The barrier is 0.06 eV lower than the two-electron reduction of CO on the perfect TiO_2 surface found in our previous work.[20] This strongly suggests that the O_v is more active for the hydrogenation of CO.

In step H-II, the HCO^- anion is then hydrogenated to CH_2O; the barrier is calculated to be 0.33 eV. (The method to align the PES of step H-I and H-II can be found in our previous

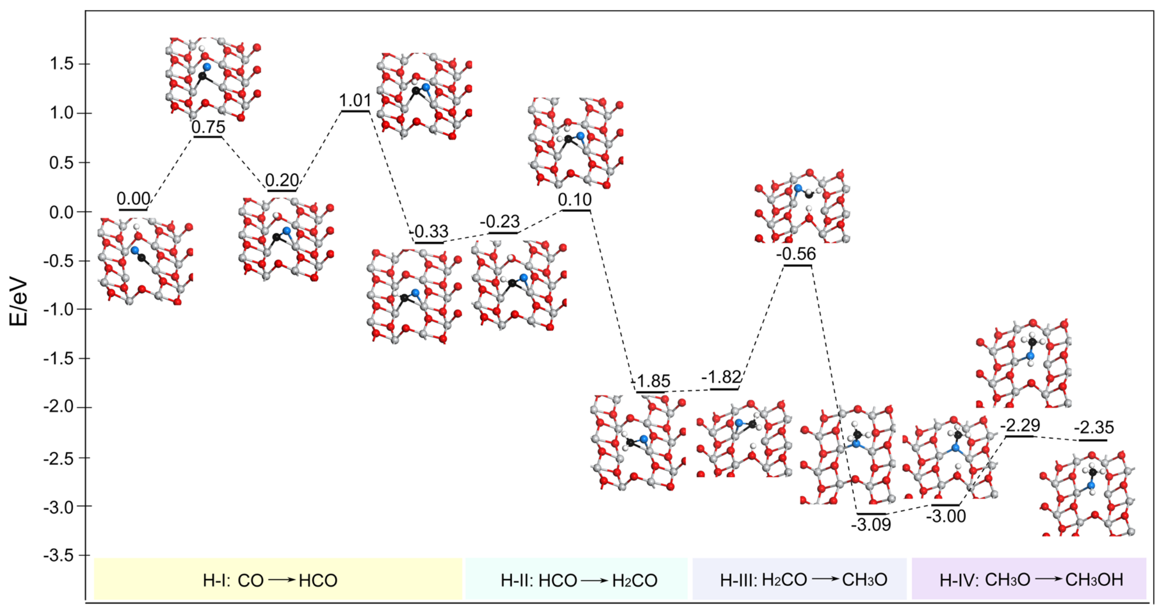

Figure 2. Full potential energy surfaces for the hydrogenation of CO to CH_3OH. Step H-I, hydrogenation of CO to HCO; step H-II HCO to CH_2O; step H-III CH_2O to CH_3O; step H-IV CH_3O to CH_3OH.

DOI: 10.1021/jacs.6b05695
J. Am. Chem. Soc. 2016, 138, 15896−15902

study and in the Supporting Information of the present work.) The adsorption energy of CH_2O at the O_v is calculated to be 2.41 eV, which is highly difficult for the molecule to desorb from it. This might be the reason why it was not detected in the experiment performed on the defective surface.[19]

In step H-III, CH_2O is reduced to $CH3O^-$ which means two electrons are also transferred. The barrier is calculated to be 1.26 eV, larger than that for the two-electron reduction of CH_2O on the perfect surface.[20] The reason might be the strong adsorption of the molecule at the O_v. A large amount of energy is required to adjust its structure to reach the proton.

At the final step (step H-IV), we found that hydrogenation of the CH_3O group to CH_3OH at the O_v is endothermic by 0.65 eV with a barrier of 0.71 eV. However, the adsorption energy of CH_3OH at the O_v is calculated to be 1.33 eV. It means that CH_3OH prefers to dissociate back to CH_3O by overcoming a small barrier of 0.06 eV. In order to form CH_3OH and CH_4, $CH_3^{\cdot}$ needs to be produced via the breaking of the C−O bond of the CH_3O group at the O_v. In this way, CH_3OH is no longer an intermediate to form $CH_3^{\cdot}$. On the contrary, it can be one of the final products as in the FdO path. The original FH/DS path can thus be modified to $CO_2 \rightarrow CO \rightarrow CH_2O \rightarrow CH_3O \rightarrow CH_3^{\cdot} \rightarrow CH_4/CH_3OH$. This new path is essentially a combination of the FH/PS and FdO/PS paths, which avoids the kinetic problem of the FH/PS path.[2,11,12]

Formation of $CH_3^{\cdot}$, CH_4, and CH_3OH. Now, we investigate the formation of $CH_3^{\cdot}$ and subsequent reactions. The PES for the formation of $CH_3^{\cdot}$ (step M-I) is shown in Figure 3. At the initial state, the CH_3O group is adsorbed as an anion $CH3O^-$ with one electron transferred from the O_v. Thus, there is still one excess electron in the system to reduce the $CH3O^-$ anion to $CH_3^{\cdot}$ radical (reaction 6). The reaction is calculated to be endothermic by 0.44 eV with a barrier of 0.63 eV. This barrier is lower than the reduction barrier of CH_3OH to $CH_3^{\cdot}$ on the perfect surface (0.95 eV),[20] which again shows that deoxygenation at the O_v is easier. The planar methyl radical has been detected by EPR measurements.[9,10] However, it was not found in the photocatalytic reaction of methanol in a recent experiment.[43] It is possible that methanol in that experiment was readily oxidized because of the absence of O_v, whereas on the defective surface the excess electrons from O_v can protect CH_3O from photooxidation and promotes its reduction.

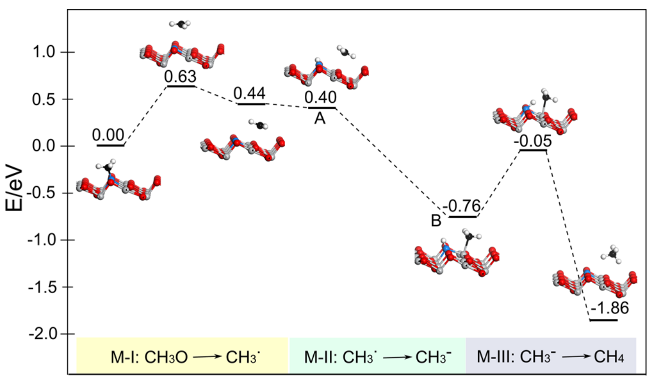

Figure 3. Formation of $CH_3^{\cdot}$ and CH_4. Step M-I, formation of $CH_3^{\cdot}$ via the breaking of the C−O bond leaving a cured O_v; step M-II, an electron transfers to $CH_3^{\cdot}$, forming a CH_3^- anion; and step M-III, the CH_3^- anion recombines with a H_b to form CH_4.

$$CH_3O^- + O_v + e^- \rightarrow CH_3^{\cdot} + O_b^{2-} \quad (6)$$

Following the FH/DS path, the $CH_3^{\cdot}$ radical can recombine with a H atom to form CH_4. This reaction should be easy due to the radical character of both species. Another possibility is that the $CH_3^{\cdot}$ radical first captures an electron to form CH_3^- (step M-II) and then recombines with a proton to give CH_4 (step M-III). In step M-II, an excess electron is injected by the adsorption of another hydrogen atom to the surface (state A in Figure 3). The $CH_3^{\cdot}$ radical can coexist with the excess electron only in the triplet state. As we force the system to be the singlet state, the electron will be transferred to the planar $CH_3^{\cdot}$ radical, forming a CH_3^- anion (state B in Figure 3) spontaneously. No transition state for this process was located in the CNEB calculation. The CH_3^- anion will then recombine with the proton to CH_4 by overcoming a barrier of 0.71 eV (step M-III). In this pathway, step M-III is the rate-limiting step to form CH_4 from CH_3O at the O_v.

As analyzed in last section, the $CH_3^{\cdot}$ radical can also be converted to CH_3OH by recombining with a OH group. If it recombines with a $^{\cdot}OH$ radical, the reaction should be easier because of the radical character of both species. However, the reduction of CO_2 to $CH_3^{\cdot}$ radical, then to CH_3OH would consume seven excess electrons and one hole (oxidize OH^- to $^{\cdot}OH$), whereas only six excess electrons are needed to reduce CO_2 to CH_3OH in principle. Thus, it is not an efficient pathway to utilize solar energy. According to our previous work,[20] the $CH_3^{\cdot}$ radical can also recombine with a OH^- to CH_3OH (reaction 7). One excess electron is released back to conduction band of TiO_2 that takes part in the reduction of other adsorbates. This reaction is exothermic by 0.67 eV with a barrier of 0.28 eV. Combining with the PES of step M-I (Figure 3), the overall barrier from CH_3O at the O_v to form CH_3OH at the Ti_{5f} is exothermic by 0.23 eV with a barrier of 0.63 eV. The barrier is slightly lower than the barrier of step M-III for the formation of CH_4 from CH_3^- anion. However, this does not mean that CH_3OH will be selectively formed from $CH_3^{\cdot}$ because it may capture an H atom to form CH_4 directly or capture an excess electron quickly to form CH_3^-(step M-II). Once the CH_3^- anion is formed, the formation barrier of CH_3OH via the recombination of the CH_3^- anion and an OH group is as high as 1.76 eV.[20] Therefore, the final selectivity toward CH_3OH or CH_4 depends on the availability of the OH group and the H (excess electron plus proton).

$$CH_3^{\cdot} + OH^- \rightarrow CH_3OH + e^- \quad (7)$$

Combining the results from Figures 1−3, the FH/DS path is modified to $CO_2 \rightarrow CO \rightarrow CH_2O \rightarrow CH_3O \rightarrow CH_3^{\cdot} \rightarrow CH_4/CH_3OH$ with the rate-limiting step to be step H-III (hydrogenation of CH_2O to CH_3O at the O_v). Its barrier is lower than that of the rate-limiting step on the perfect surface (1.41 eV).[20] It indicates that the O_v is more active than Ti_{5f} for the reaction along the FH path.

FdO Path. The first step of the FdO path is the same as that of the FH path, i.e., the deoxygenation of CO_2 to CO. In the FdO path, CO is proposed to further dissociate to give $C^{\cdot}$ radical. However, as presented below, our calculations show that it is energetically unfavorable on both the perfect and the defective surfaces.

On the perfect TiO_2 surface, we first consider the direct dissociation of CO into C and O atoms adsorbed at two adjacent Ti_{5f} sites. However, we find that the C atom will extract a lattice oxygen to form an adsorbed CO (Figure 4 A), suggesting that the FdO path can not proceed on the perfect surface. Then, we consider the dissociation of CO at the O_v,

DOI: 10.1021/jacs.6b05695
J. Am. Chem. Soc. 2016, 138, 15896−15902

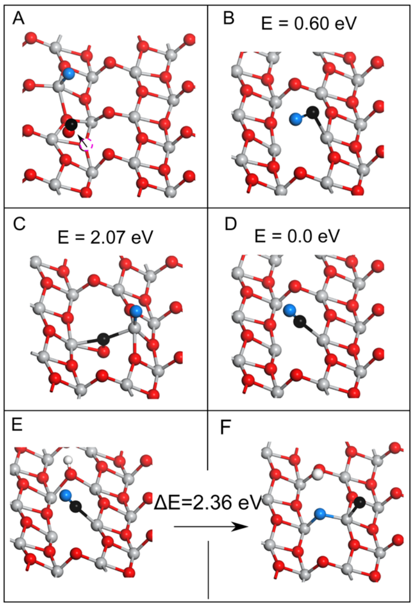

Figure 4. Adsorption of and dissociation of CO. In structure A, the pink dashed oxygen is extracted by the C atom leaving a vacancy there. The energy of structure D is taken as zero for the relative energies between structures B–D. The process E–F is endothermic by 2.36 eV.

resulting in a cured O_v and a C atom adsorbed on the nearby Ti_{5f} atom. The C atom is found to recombine with the oxygen, forming a CO adsorbed at the O_v (Figure 4 B). We even consider the case in which CO dissociates at the O_v with C adsorbed at the O_v and O on the nearby Ti_{5f}. We find that the C atom could form C–O bond with a subsurface O (Figure 4 C) with an energy of 2.07 eV higher than the adsorption of CO at the O_v (Figure 4 D). We succeed to obtain a surface carbon species when there is another H adsorbed on the surface, implying that CO can dissociate when the surface has three excess electrons (two from O_v and one from H). However, the dissociation in this case (Figure 4E,F) is highly endothermic by 2.36 eV. It can be concluded from all these results that it is highly impossible to form an adsorbed C radical from the dissociation of CO molecule.

It seems that the FdO path can proceed neither on the perfect surface nor at the O_v. However, CO adsorbed at the O_v is stoichiometrically equivalent to C adsorbed on perfect TiO_2. Hydrogenation of adsorbed C to CH_3 is stoichiometrically equivalent to hydrogenation of CO adsorbed at the O_v to CH_3O. In this sense, the FdO/PS path is essentially equivalent to FH/DS path. As discussed in the next section, by considering that the reaction can proceed via both the FH/PS and FH/DS paths, we are able to propose a simple mechanism for the reaction which is compatible with various experiments.

New Mechanism and the Selectivity of the Reaction. Combined with our previous study,[20,29] we propose a new mechanism by just considering FH path at both Ti_{5f} and O_v sites. As shown in the Scheme 2, if CO_2 is adsorbed at the Ti_{5f} site, then the reaction follows the FH/PS path (The formation of HCOOH is also included as another branch); if CO_2 diffuses to O_v, then the reaction changes to the FH/DS path. The interwinding of both paths is also allowed: If CO_2 dissociates at the O_v produce a CO adsorbed at the Ti_{5f}, then the reaction is changed back to FH/PS path; if CO_2 is deoxygenated via the process in Figure 1b or if any of the intermediates in FH/PS path occupies another O_v, then the reaction will change back to the FH/DS path.

Scheme 2. New Mechanism for the Photoreduction of CO_2[a]

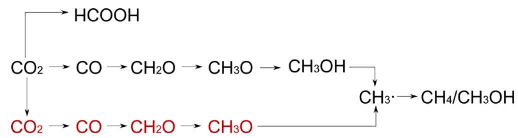

[a]Red species are adsorbed at oxygen vacancy and black ones on surface Ti.

The FH/PS path is thermodynamically feasible. HCOOH, CH_2O, and CH_3OH can be produced via this path.[44] However, these intermediates adsorbed at the Ti_{5f} site are readily oxidized by photogenerated hole rather than reduced by electron.[20,29,43] The interwinding of the oxidation and reduction reaction results in low efficiency. This maybe the reason why they are usually not the major products. However, because the availability of the photogenerated electron and holes are quite sample-dependent, the final product of the reaction may become unpredictable. This may be why there are no experiments showing that the reaction follows exactly the FH/PS path.

For the FH/DS path, deoxygenation becomes easier at the O_v. Furthermore, O_v can provide two excess electrons that can protect the intermediates from the photooxidation and promote them for further reduction. For example, in steps H-I and H-III, two electrons are transferred in each step. This is also consistent with the recent experiment, which showed that formaldehyde can only serve as hole scavengers or be reduced via two-electron processes.[43] These also explain why the defective TiO_2 was found to be more active than perfect ones.[19] In contrast, the intermediates CH_2O and CH_3O of the FH/DS path are strongly adsorbed at the O_v; CH_3OH and CH_4 can only be produced from $CH_3^{\cdot}$ which is formed via the breaking of C–O bond of CH_3O adsorbed at the O_v. These make the reaction path appear to be the FdO path. In fact, the FH/DS path is stoichiometrically equivalent to the FdO/PS path. It is compatible with the experiments that support the FdO/PS path.[11] We notice that FH/DS path is also similar to that for the electrochemical reduction of CO_2 on the Cu(111) surface,[45] which seems to further suggest that it may be a general one for the reduction of CO_2.

To comprehensively understand the selectivity of the reaction, we need to consider the FH path at both Ti_{5f} site and O_v. For those samples with low density of O_v, traces of HCOOH, CH_2O, and CH_3OH should be observed with low efficiency[44] because they can be easily oxidized. HCOOH has been found to be the main product in some experiments. However, they are conducted in liquid[46] or super critical[47] CO_2. It is probably the reaction equilibrium protects HCOOH from being oxidized back to CO_2. On the defective surface, CO can be produced from CO_2 adsorbed at the Ti_{5f} site and O_v especially the latter because the deoxygenation becomes easier.[19] It may not appear in all experiments because it is strongly adsorbed on the surface and oxidized back to CO_2 by O_2 from water oxidation.[11,12] For CH_3OH and CH_4, they do not appear consecutively probably because they are produced via FH/DS path,[11] and the final product is probably determined by the availability of OH and H as discussed above.[7] In real experiments, the reaction can proceed via both pathways. Ti_{5f} on the surface is abundant, but the amount of O_v depends

DOI: 10.1021/jacs.6b05695
J. Am. Chem. Soc. 2016, 138, 15896–15902

greatly on the preparation method, leading to the sample-dependent product distribution. Based on the features of both pathways, the final product distribution depends also on the experimental details that affect the availability of photo-generated holes and electrons[7] and the availability of OH and H. Our proposed mechanism is indeed compatible with different experiments. The key point here is that the FH/DS path is the combination of FH/PS and FdO/PS paths.

We can see that O_v plays a very important role in the new mechanism. The total reaction in our calculations can be presented as

$$CO_2 + 8e^- + 4H^+ + 2O_v \rightarrow CH_4 + 2O_b^{2-} \quad (8)$$

In addition to four protons and four photogenerated electrons, two O_v and four excess electrons from TiO_2 are consumed in this process. To complete the photocatalytic cycle, O_v and excess electrons should be restored after the reaction. Fujishima et al.[48] and Tseng et al.[49] have proposed that O_v can be generated under UV illumination during the generation of O_2:

$$2O_b^{2-} + 4h^+ \rightarrow O_2 + 2O_v \quad (9)$$

In a recent theoretical study, Selloni et al.[32] has showed that H_2O is oxidized to O_2 by the hole to generate O_v:

$$H_2O + 4h^+ + O_b^{2-} \rightarrow 2H^+ + O_2 + O_v \quad (10)$$

It is clear that O_v can be regenerated in the oxidation part of the overall artificial photosynthesis reaction, and the excess electrons of TiO_2 will be restored by photogenereated electrons.

If the O_v produced from reaction 10 is occupied by another H_2O that can be dissociated to cure it and produce two adsorbed protons

$$H_2O + O_v \rightarrow 2H^+ + O_b^{2-} \quad (11)$$

then the total reaction for water oxidation (reactions 10 + 11) becomes reaction 1. An artificial photosynthesis cycle can be completed either by coupling reaction 1 with the FH/PS path or by coupling reaction 10 with the FH/DS path. One may have noticed that the FH/DS path can also take place on the perfect surface if O_v is produced in water oxidation via reaction 10. Thus, the higher activity of the defective surface[19] can only be attributed to the abundance of O_v at the initial stage of the reaction for the strong adsorption and the reduction of CO_2. If O_v is not recovered efficiently during the reaction, then the activity of the catalyst will be decreased.[50] Therefore, it is desirable to design new catalysts that easily lose the surface oxygens. For example, the enhancement of the activity of TiO_2 can be attributed to the promotion of formation of O_v by Cu deposition[51] or sulfuric acid modification.[52] However, the easier to lose the lattice oxygen, the harder to deoxygenate the adsorbate. Rational design of better material must find the balance between these two aspects, but the excess electrons are essential for the reduction of the intermediates. It is better to leave the catalyst as a n-type semiconductor after the modification.

It is noticed that the formation of C2 molecules has not been specifically discussed in our mechanism, which is mainly because they are not the major products in the experiments. In fact, C2 molecules can be formed via the coupling of the C1 intermediates in our proposed mechanism. For example, two formyl radicals adsorbed on the surface can dimerize to glyoxal;[53] the coupling of methyl radical with other intermediates may even yield other higher carbon molecules.[54] The glyoxal can also be transformed back to CH_4. However, this pathway cannot explain the formation of formaldehyde and methanol, which are the major products of many experiments. It also allows the intertwining of photooxidation and photo-reduction processes, which will result in lower efficiency.[2] Part of potential energy surface of the glyoxal pathway has been investigated at GGA level by a recent calculation.[55] More general discussion on the formation of C2 molecules can be found in the recent review.[54]

CONCLUSIONS

We have systematically investigated the photocatalytic reduction of CO_2 on the perfect and defective anatase $TiO_2(101)$ surfaces following both the fast-hydrogenation and fast-deoxygenation pathways. We have found that the oxygen vacancy is more active than the surface Ti atom for the reaction. The fast-hydrogenation path at the oxygen vacancy is modified to a new one which is a combination of the fast-hydrogenation and fast-deoxygenation paths. Our calculated results suggest that the fast-deoxygenation can proceed neither on the perfect surface nor on the defective surface because the formation of the key intermediate C˙surface is energetically unfavorable. We propose a new mechanism in which the fast-hydrogenation path can occurs at both the surface Ti and the oxygen vacancy to explain various experiments and rationalize the selectivity of the reaction. This mechanism greatly simplifies our understanding of photocatalytic reduction of CO_2 and also enables us to propose a strategy to design better photocatalysts.

ASSOCIATED CONTENT

Supporting Information

This material is available free of charge via the Internet at http://pubs.acs.org/. The Supporting Information is available free of charge on the ACS Publications website at DOI: 10.1021/jacs.6b05695.

Results in Figures 1−4 with pure GGA+U method; method for the alignment of the potential energy surfaces when we add H to the system; All the optimized structures and their absolute energies in the main text. (PDF)

Optimized structures for compounds **1**−**4** (CIF)

AUTHOR INFORMATION

Corresponding Author

*E-mail: yiluo@ustc.edu.cn

ORCID

Yongfei Ji: 0000-0002-6759-7126

Notes

The authors declare no competing financial interest.

ACKNOWLEDGMENTS

This work was supported by the National Natural Science Foundation of China (21421063, 21633007), the Strategic Priority Research Program of the Chinese Academy of Sciences (XDB01020200), the Göran Gustafsson Foundation for Research in Natural Sciences and Medicine, and the Swedish Research Council (VR). The Swedish National Infrastructure for Computing (SNIC) is acknowledged for computer time.

REFERENCES

(1) Mao, J.; Li, K.; Peng, T. Y. *Catal. Sci. Technol.* **2013**, *3*, 2481–2498.
(2) Habisreutinger, S. N.; Schmidt-Mende, L.; Stolarczyk, J. K. *Angew. Chem., Int. Ed.* **2013**, *52*, 7372–7408.
(3) Dhakshinamoorthy, A.; Navalon, S.; Corma, A.; Garcia, H. *Energy Environ. Sci.* **2012**, *5*, 9217–9233.
(4) Kondratenko, E. V.; Mul, G.; Baltrusaitis, J.; Larrazabal, G. O.; Perez-Ramirez, J. *Energy Environ. Sci.* **2013**, *6*, 3112–3135.
(5) Liu, L.; Li, Y. *Aerosol Air Qual. Res.* **2014**, *14*, 453–469.
(6) Izumi, Y. *Coord. Chem. Rev.* **2013**, *257*, 171–186.
(7) Kocí, K.; Obalova, L.; Lacny, Z. *Chem. Pap.* **2008**, *62*, 1–9.
(8) White, J. L.; Baruch, M. F.; Pander Iii, J. E.; Hu, Y.; Fortmeyer, I. C.; Park, J. E.; Zhang, T.; Liao, K.; Gu, J.; Yan, Y.; Shaw, T. W.; Abelev, E.; Bocarsly, A. B. *Chem. Rev.* **2015**, *115*, 12888–12935.
(9) Anpo, M.; Yamashita, H.; Ichihashi, Y.; Ehara, S. *J. Electroanal. Chem.* **1995**, *396*, 21–26.
(10) Dimitrijevic, N. M.; Vijayan, B. K.; Poluektov, O. G.; Rajh, T.; Gray, K. A.; He, H.; Zapol, P. *J. Am. Chem. Soc.* **2011**, *133*, 3964–3971.
(11) Kocí, K.; Obalova, L.; Solcova, O. *Chem. Process Eng.* **2010**, *31*, 395–407.
(12) Tan, S. S.; Zou, L.; Hu, E. *Catal. Today* **2008**, *131*, 125–129.
(13) Diebold, U. *Surf. Sci. Rep.* **2003**, *48*, 53–229.
(14) Brookes, I. M.; Muryn, C. A.; Thornton, G. *Phys. Rev. Lett.* **2001**, *87*, 266103.
(15) Petrik, N. G.; Kimmel, G. A. *J. Phys. Chem. Lett.* **2010**, *1*, 2508–2513.
(16) Zhou, C.; Ren, Z.; Tan, S.; Ma, Z.; Mao, X.; Dai, D.; Fan, H.; Yang, X.; LaRue, J.; Cooper, R.; Wodtke, A. M.; Wang, Z.; Li, Z.; Wang, B.; Yang, J.; Hou, J. *Chem. Sci.* **2010**, *1*, 575–580.
(17) Hoang, S.; Berglund, S. P.; Hahn, N. T.; Bard, A. J.; Mullins, C. B. *J. Am. Chem. Soc.* **2012**, *134*, 3659–3662.
(18) Nowotny, M. K.; Sheppard, L. R.; Bak, T.; Nowotny, J. *J. Phys. Chem. C* **2008**, *112*, 5275–5300.
(19) Liu, L. J.; Zhao, H. L.; Andino, J. M.; Li, Y. *ACS Catal.* **2012**, *2*, 1817–1828.
(20) Ji, Y.; Luo, Y. *ACS Catal.* **2016**, *6*, 2018–2025.
(21) Kresse, G.; Hafner, J. *Phys. Rev. B: Condens. Matter Mater. Phys.* **1993**, *47*, 558–561.
(22) Kresse, G.; Furthmuller, J. *Comput. Mater. Sci.* **1996**, *6*, 15–50.
(23) Kresse, G.; Furthmuller, J. *Phys. Rev. B: Condens. Matter Mater. Phys.* **1996**, *54*, 11169–11186.
(24) Kresse, G.; Hafner, J. *Phys. Rev. B: Condens. Matter Mater. Phys.* **1994**, *49*, 14251–14269.
(25) Kresse, G.; Joubert, D. *Phys. Rev. B: Condens. Matter Mater. Phys.* **1999**, *59*, 1758–1775.
(26) Blöchl, P. E. *Phys. Rev. B: Condens. Matter Mater. Phys.* **1994**, *50*, 17953–17979.
(27) Perdew, J. P.; Burke, K.; Ernzerhof, M. *Phys. Rev. Lett.* **1996**, *77*, 3865–3868.
(28) Ji, Y.; Luo, Y. *J. Phys. Chem. C* **2014**, *118*, 6359–6364.
(29) Ji, Y.; Wang, B.; Luo, Y. *J. Phys. Chem. C* **2014**, *118*, 21457–21462.
(30) Henkelman, G.; Jonsson, H. *J. Chem. Phys.* **2000**, *113*, 9978–9985.
(31) Valdés, A.; Qu, Z. W.; Kroes, G. J.; Rossmeisl, J.; Nørskov, J. K. *J. Phys. Chem. C* **2008**, *112*, 9872–9879.
(32) Li, Y.-F.; Selloni, A. *ACS Catal.* **2016**, *6*, 4769–4774.
(33) Uner, D.; Oymak, M. M. *Catal. Today* **2012**, *181*, 82–88.
(34) He, H. Y.; Zapol, P.; Curtiss, L. A. *Energy Environ. Sci.* **2012**, *5*, 6196–6205.
(35) Tamaki, Y.; Furube, A.; Murai, M.; Hara, K.; Katoh, R.; Tachiya, M. *Phys. Chem. Chem. Phys.* **2007**, *9*, 1453–1460.
(36) Tamaki, Y.; Furube, A.; Katoh, R.; Murai, M.; Hara, K.; Arakawa, H.; Tachiya, M. *C. R. Chim.* **2006**, *9*, 268–274.
(37) Mori-Sánchez, P.; Cohen, A. J.; Yang, W. *Phys. Rev. Lett.* **2008**, *100*, 146401.
(38) Dudarev, S. L.; Botton, G. A.; Savrasov, S. Y.; Humphreys, C. J.; Sutton, A. P. *Phys. Rev. B: Condens. Matter Mater. Phys.* **1998**, *57*, 1505–1509.
(39) Heyd, J.; Scuseria, G. E.; Ernzerhof, M. *J. Chem. Phys.* **2003**, *118*, 8207–8215.
(40) Sorescu, D. C.; Al-Saidi, W. A.; Jordan, K. D. *J. Chem. Phys.* **2011**, *135*, 124701.
(41) Gattrell, M.; Gupta, N.; Co, A. *J. Electroanal. Chem.* **2006**, *594*, 1–19.
(42) Xu, M. C.; Noei, H.; Buchholz, M.; Muhler, M.; Woll, C.; Wang, Y. M. *Catal. Today* **2012**, *182*, 12–15.
(43) Dimitrijevic, N. M.; Shkrob, I. A.; Gosztola, D. J.; Rajh, T. *J. Phys. Chem. C* **2012**, *116*, 878–885.
(44) Inoue, T.; Fujishima, A.; Konishi, S.; Honda, K. *Nature* **1979**, *277*, 637–638.
(45) Peterson, A. A.; Nørskov, J. K. *J. Phys. Chem. Lett.* **2012**, *3*, 251–258.
(46) Kaneco, S.; Kurimoto, H.; Ohta, K.; Mizuno, T.; Saji, A. *J. Photochem. Photobiol., A* **1997**, *109*, 59–63.
(47) Kaneco, S.; Kurimoto, H.; Shimizu, Y.; Ohta, K.; Mizuno, T. *Energy* **1999**, *24*, 21–30.
(48) Fujishima, A.; Rao, T. N.; Tryk, D. A. *J. Photochem. Photobiol., C* **2000**, *1*, 1–21.
(49) Tseng, Y. H.; Kuo, C. S.; Huang, C. H.; Hirakawa, T.; Negishi, N.; Bai, H. L. *Micro Nano Lett.* **2010**, *5*, 81–84.
(50) Liu, L.; Zhao, C.; Li, Y. *J. Phys. Chem. C* **2012**, *116*, 7904–7912.
(51) Zhu, S.; Liang, S.; Tong, Y.; An, X.; Long, J.; Fu, X.; Wang, X. *Phys. Chem. Chem. Phys.* **2015**, *17*, 9761–9770.
(52) He, Z.; Tang, J.; Shen, J.; Chen, J.; Song, S. *Appl. Surf. Sci.* **2016**, *364*, 416–427.
(53) Shkrob, I. A.; Marin, T. W.; He, H. Y.; Zapol, P. *J. Phys. Chem. C* **2012**, *116*, 9450–9460.
(54) Karamian, E.; Sharifnia, S. *J. CO2 Util.* **2016**, *16*, 194–203.
(55) Ip, C. M.; Troisi, A. *Phys. Chem. Chem. Phys.* **2016**, *18*, 25010–25021.

DOI: 10.1021/jacs.6b05695
J. Am. Chem. Soc. 2016, 138, 15896–15902